Bioscene

Synthesis of Zinc Oxide Nanoparticles with Neem Flowers Extract and its Applications

Thiruppathy J[1], S Selvarani[2], Vignesh TK[3]

[1]Assistant professor, department of chemistry, Thiagarajar college, Madurai, Tamilnadu, India
[2]Assistant professor, department of zoology, Thiagarajar college, Madurai, Tamilnadu, India
[3]Research scholar, Thiagarajar college, Madurai, Tamilnadu, India

Abstract: In this study planned to synthesize ZnONPs biologically with Neem flower extract to predict the effect of the antibacterial and antifungal activities. Synthesised ZnONPs with neem flowers extract were characterized by UV–visible spectroscopy (UV–vis), X-ray diffractometer (XRD), Fourier transform infrared spectroscopy (FT-IR), Scanning electron microscopy (SEM) and EDAX. This study also covered photocatalytic degradation activity by (UV-vis). The crystalline structure of ZnONPs were shown by XRD studies. SEM studies gave an idea of agglomeration of particles. The maximum zone of inhibition was obtained in both antibacterial and antifunal activities of ZnONPs with neem flowers extract. using disc diffusion method..

Keywords: ZnO nanoparticles(NPs), neem flowers extract(NFE), photocatalytic degradation activity, antibacterial and antifungal activity

1. Introduction

Antibacterial agents are compounds used to inhibit bacterial growth and their modus operandi interrupts replication, transcription, and translation in the cell. It deteriorates the metabolic process of the bacteria and ends with mortality. These antibacterial agents have several industrial applications such as textiles, dermatological therapies, dental composites, food packaging and medicine that are of increasing demand nowadays. Several studies have reported that the use antibiotics has led to the emergence of multidrug-resistant bacterial strains. In recent development of science and technology, water pollution makes significant problem in the world. To degrade the organic pollutants in water using photo catalytic activity and also by mixing with natural leaves extract. There is another method to degrade water pollutants are photo catalyst [1,2] For example cerium oxide nanoparticles have been used as photocatalyst in several ways[3], optical film material [4], auto-motive exhaust catalyst [5], ultraviolet shielding material [6], gas sensors, optoelectronics and microelectronics [7]. Due to the bandgap of 3.2 eV makes CeO_2 an efficient adsorbent in UV region and effective photocatalyst. In some cases nanoparticles of

CeO_2 havebeen projected   for the conventional TiO_2 to the stidy of photocatalyst[8].CeO_2 nanoparticles have been used as degrade methylene blue[9]. Manganese-doped cerium oxide nanoparticleshave been widely explored inenvironmental remediation for wastewatertreatment in particularly acridine orange under UV light [10], congo red [11], rhodamine-Bdye using visible light [12]. CeO_2allows only 3-5% of solar energy consists of UV-radiation due to its large band gap[13] . According to thesurface defect method that itprevents recombination of electron and holes. In addition,it adsorbs dye molecules for degradation and increase photocatalytic activity [14]. Transition metal ions likeFe [15], Au [16], Pd- [17], Mn [18], doped with CeO_2nanoparticles.The doping of Mn ion with CeO_2 nanoparticles causes decrease in band gap and lowering energy of empty d-orbitals in Mn than 4f orbitals of Ce [19]. The 4f electronic configuration can enhance transfer of an electron from the adsorbeddye to oxygen species, thus increases the photocatalytic activity [20 The photocatalytic activity of ZnO NPs have beeninvestigated towards the degradation of anthraquinone dyeremazol brilliant blue R under visible and UV irradiation. Remazol brilliant blue R is a reactive dye that contains alkylsulphonate group. but its non-biodegradability harms aquatic life [21].ZnO nanoparticles (ZnO-NPs) are becoming increasingly important in the health industry for the following reasons, unique antimicrobial and wound healing ability, UV filtration capacity, high catalytic and photochemical activities [22]. ZnO nanoparticles antibacterial activity arises from   large concentration of H_2O_2, obtained from the surface of the nanoparticles. During the synthesis of conventional ZnONPs involvesusuage of zinc nitrate , it has a moderate health warning and a strong oxidizer.To restrict this one by   avoiding the use of zinc nitrate inZnONPs production[23].The photo degradation studies were carried out by ZnO NPs are reported[24].In this study toinvestigate the effect ofZnO Nanoparticles doped with neem flowers extract synthesized by coprecipitation method.

2. Experimental action
2.1Green synthesis of ZnO nanoparticles
0.06M(10.99g) 0f Zinc acetate(Zn(COCH3)$_2$.2H$_2$O) is mixed with 300ml of ethanol stirred vigorsouly for 1hour and 0.2M(17.71g) of oxalic acid(COOH)$_2$ is mixed with 200ml of ethanol stirred for 1 hour. Then mixed the two solution slowly. A White gelatinous precipitate was obtained. Which was dried under vacuum at 90℃ for 2 hour and then calcinated at different temperatures.Neem flowers extract is prepared from 25g of neem flowers grind in mortar then take the flowers in beaker add 100 ml of water heated and filtered. The Zinc oxide powder is dissolved in dilute HNO3 and then add1% and 2% neem flowers extract..
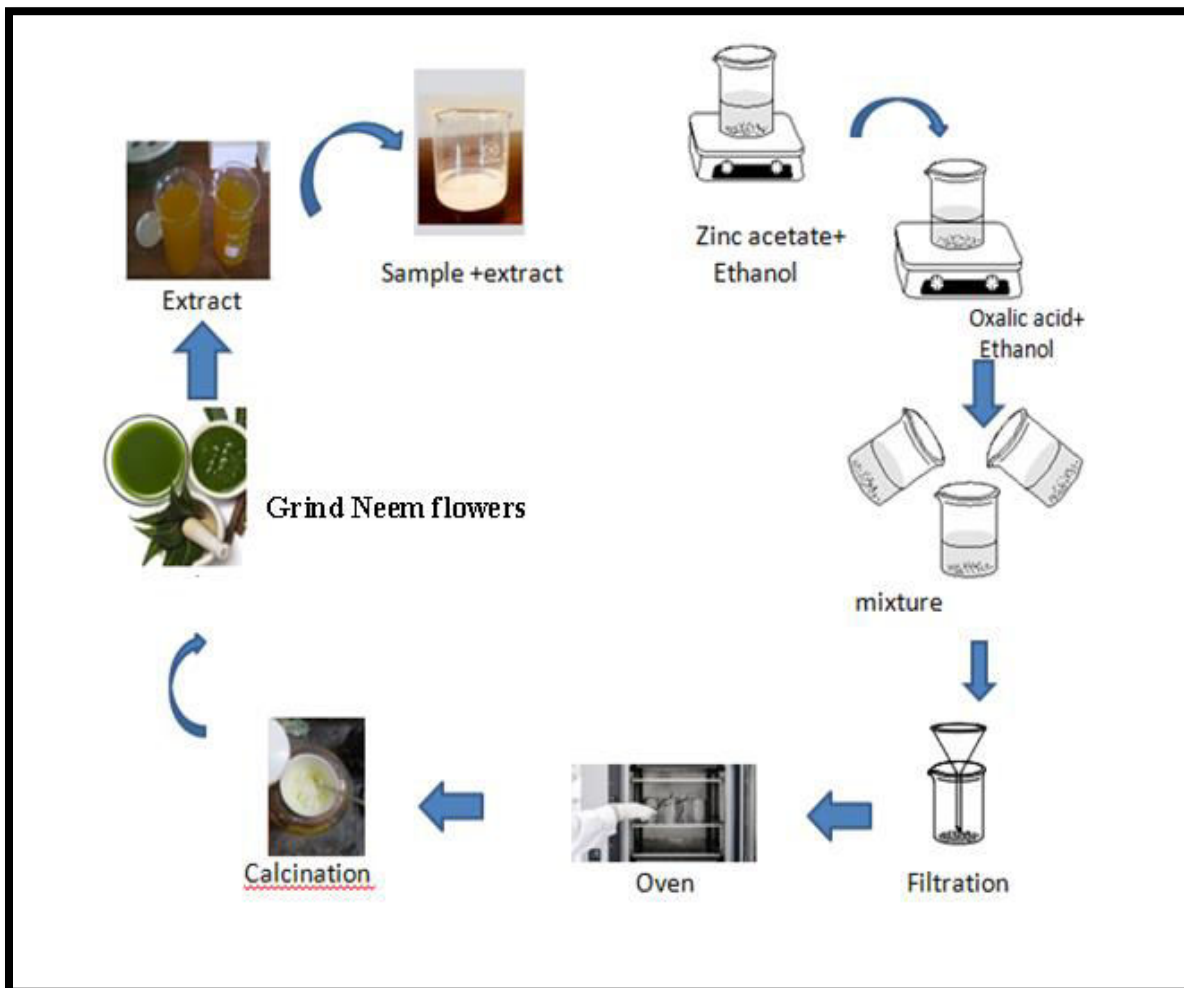
2.2 Graphical abstract

Fig 1. Graphical abstract of green synthesis of ZnONPs with neem flowers extract

3. Result and discussion
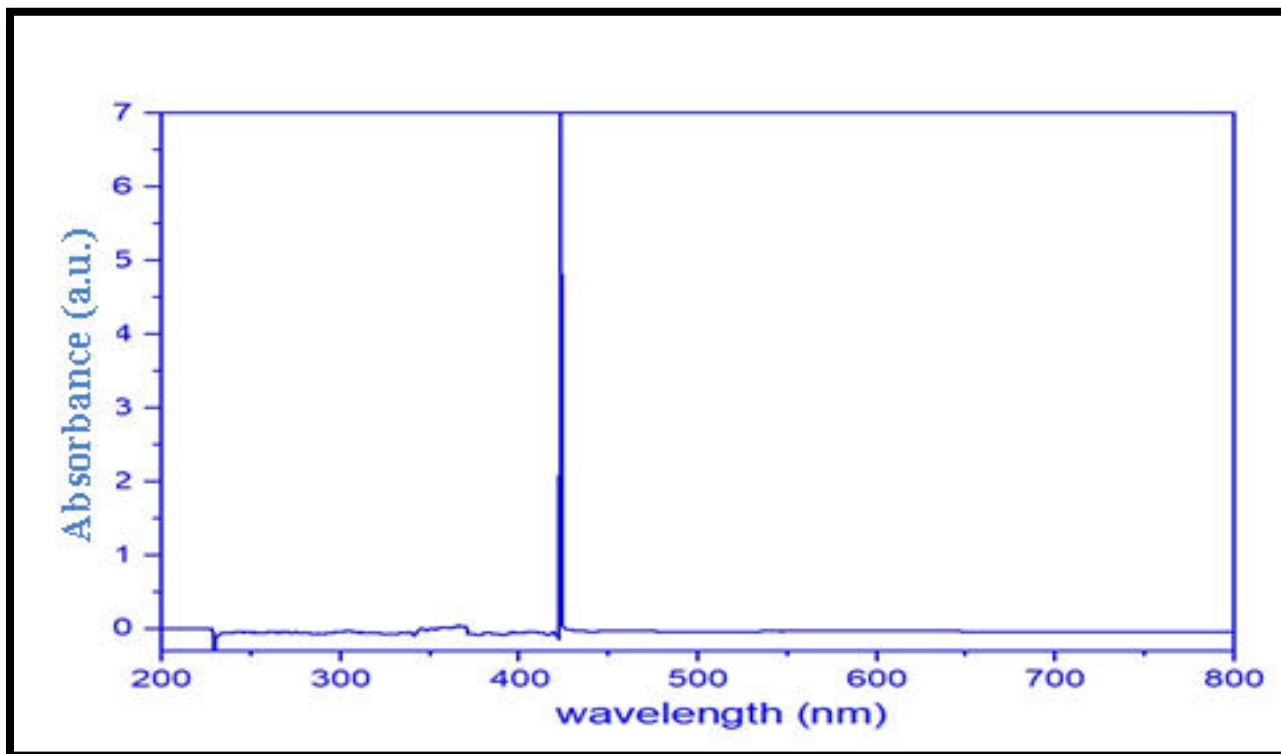### 3.1 UV-Visible Spectroscopy

Fig2. UV- Visible spectroscopy

Optical properties were studied by UV–Visible spectrophotometer in the range of 190 nm–1100 nm. From (Fig. 2 for pure zinc oxide nanoparticles the absorption edge was observed in the UV (410 nm) region. It reveals that, while adding ZnO with neem flowers extract in methyl red dye the optical properties of Zinc oxide nanoparticles have been enhanced. Furthermore, peak positions indicate that shift in the UV region was due to their change in size of the synthesized nanoparticles associated with neemflowers extract.After the addition of ZnONanaoparticles with neem flowers extract 1M and 2M in methyl red dye, its absorbance decreased.

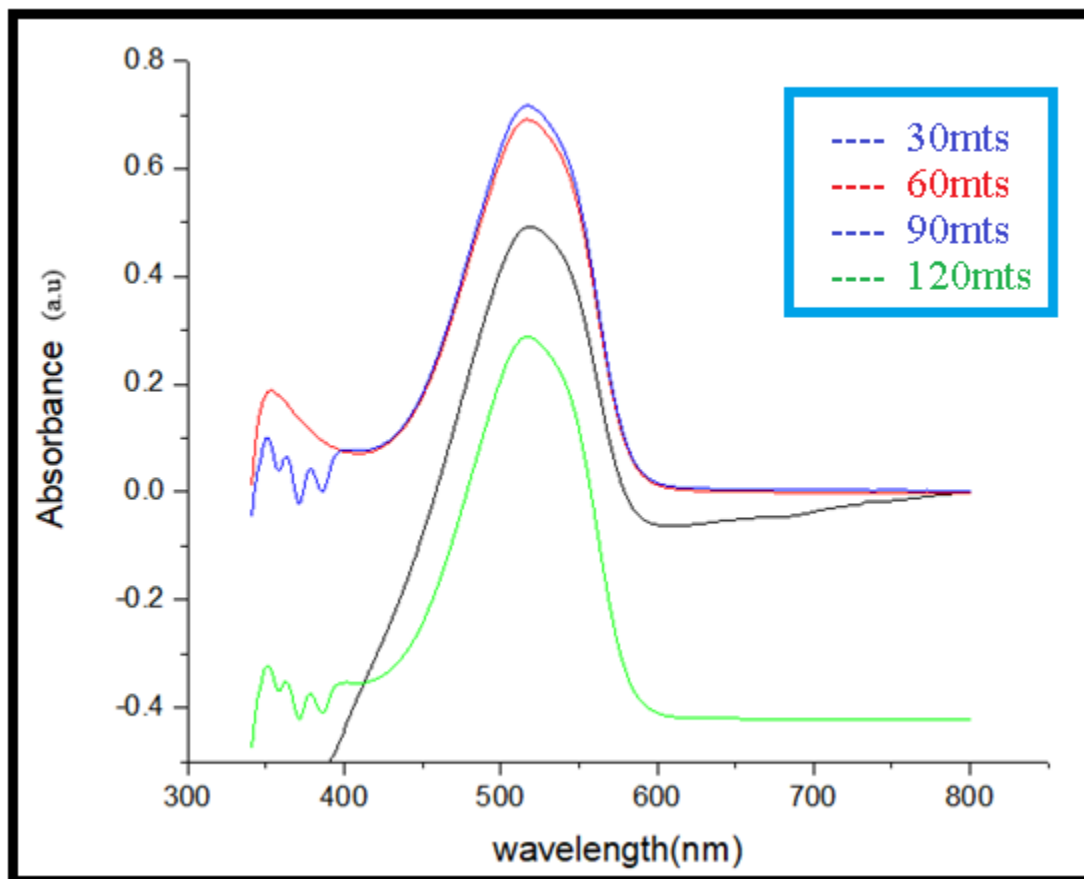### 3.2 Photo degradation curve

Fig 3. Photodegradation curves of ZnO with Neem flowers extract nanoparticles

The visible light source is a 350 W xenon lamp with JASCO-V730 ultraviolet cutoff filter and visible light reflection filter (through 420–780 nm visible light). The produced materials photocatalytic activity was assessed using methyl red as the target pollutant dye. The photocatalytic activity of the green synthesized sample was investigated for the degradation of methyl red dye under visible and ultraviolet (UV) irradiation. In the proper steps in photo catalytic process, 2.5 mg of a sample which was taken as photocatalyst and added in touch with 10 ml of purely dissolved in water medium of methyl red. The whole data of photocatalytic activity was observed in a photoreactor equipped with preliminary adjustment of lamp intensity at 6.0mW cm^{-2} placed at a distance 25 cm as well as inbuilt stirrer and 25 °C constant temperature maintained using coolant setup. The photodegradation of the methyl red dye was surveillance at regular intervals by their maximum strong absorbance and minimum weak absorbance at ~ 340 and ~ 510 nm, respectively, using the

above photoreactor.After the addition of ZnONanaoparticles with neem flowers extract its absorbance will be decreased after 30 mts,60 mts,90 mts,and 120 mts from figure 3. The effect of dye nature reduced after running for several hours.Generally,the bandgap energy of ZnO is approximately 3.37 eV at room temperature. But, the addition of ZnO NPs with neem flowers extract in methyl red the bandgap energy is decreased to 2.93 eV, it is shown in the figure 4[25-27]. Due to this decrease in bandgap energy photo catalytic efficiency is worked out.The maximum photo catalytic efficiency is obtained bythe addition of 2MZnONFE solution in methyl red dye.
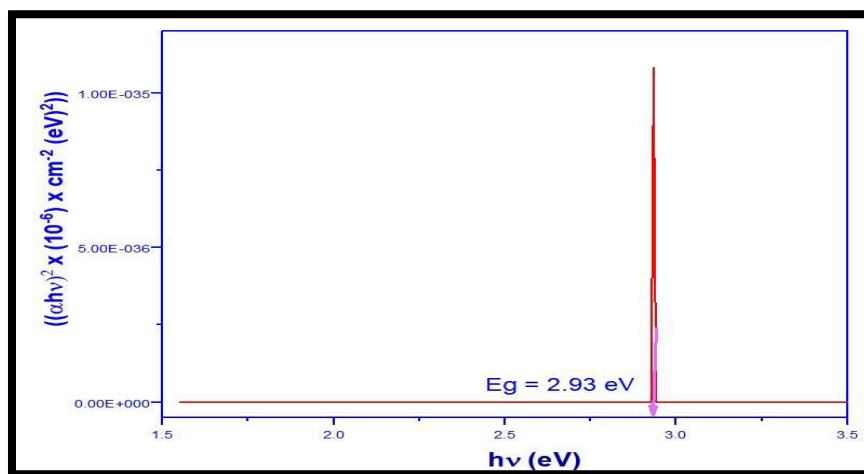

Fig 4. Bandgap energy curve of ZnO with Neem flowers extract nanoparticles
The photocatalytic efficiency is calculated by the equation (1)
$$D (\%) = C_o-C/ C_o ----------------------------(1)$$
Where, C_o is the initial concentration of methylred solution and C is its final concentration after degradation. A series of experiments are carried out by degrade dye with adsorption by adding ZnONPs with NFE in methylred and blank sample without degradation.

.3.3.Antimicrobial and Antifungal activities
3.3.1 Antimicrobial activity
The antimicrobials present in the given sample were allowed to diffuse out into the medium and interact in a plate freshly seeded with the test organisms. The resulting zones of inhibition will be uniformly circular as there will be a confluent lawn of growth. The diameter of zone of inhibition can be measured in millimeters. (E.coli-443 and Staphylococcus aureus- 902) was purchased from MTCC, Chandihar, India. Nutrient Agar medium, Nutrient broth, Gentamicin antibiotic solution was purchased from Himedia, India. Test samples, petri-plates, test tubes, beakers conical flasks were from Borosil, India. Spirit lamp, double distilled water.

3.3.2Agar-well diffusion method

The medium was prepared by dissolving 2.8 g of the commercially available Nutrient Agar Medium (HiMedia) in 100ml of distilled water. The dissolved medium was autoclaved at 15 lbs pressure at 121°C for 15 minutes. The autoclaved medium was mixed well and poured onto 100mm petriplates (25-30ml/plate) while still molten.

Nutrient broth was prepared by dissolving 2.8 g of commercially available nutrient medium (HiMedia) in 100ml distilled water and boiled to dissolve the medium completely. The medium was dispensed as desired and sterilized by autoclaving at 15 lbs pressure (121°C) for 15 minutes. Petri plates containing 20 ml nutrient agar medium were seeded with 24 hr culture of bacterial strains were adjusted to 0.5 OD value according to McFarland standard, (E.coli-443 and Staphylococcus aureus-902)Wells were cut and concentration of sample Extract (500, 250, 100 and 50 μg/ml) was added. The plates were then incubated at 37°C for 24 hours. The antibacterial activity was assayed by measuring the diameter of the inhibition zone formed around the wells. Gentamicin antibiotic was used as a positive control. The values were calculated using Graph Pad Prism 6.0 software (USA).
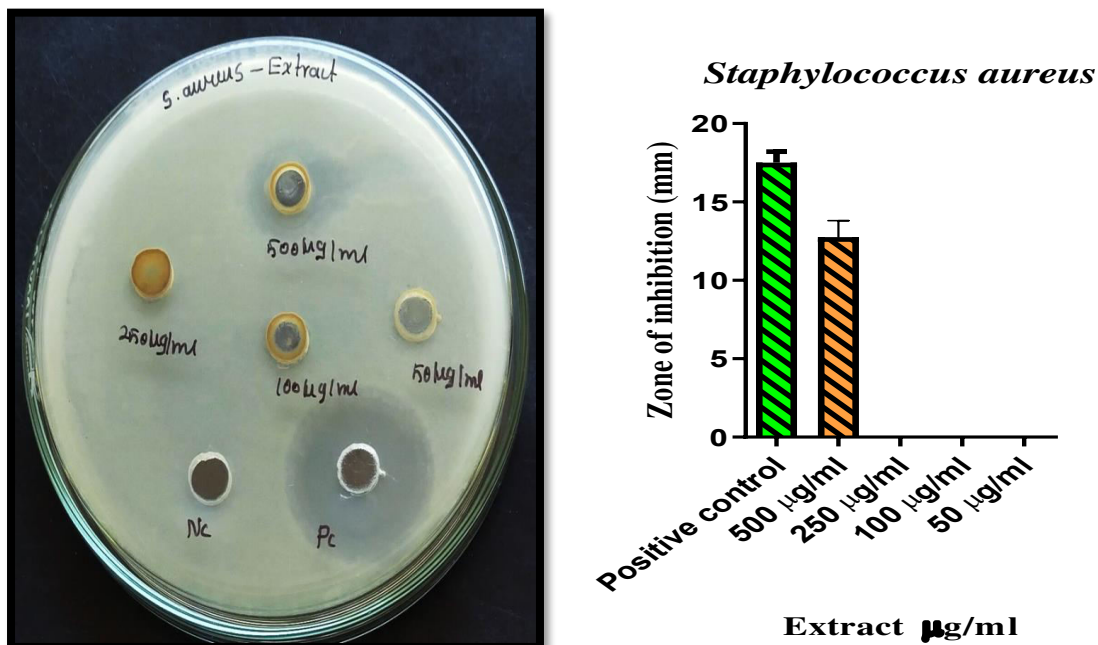

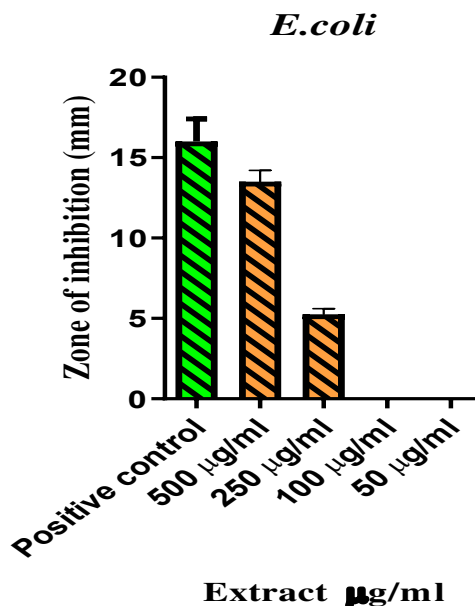Fig 5.Effect of sample Extract against Staphylococcus aureus and its bar diagram

Fig 6.Effect of sample Extract against E-coli and its bar diagram

Table 1. Means ± SD of zone of inhibition obtained by sample Extract againstE.coliand Staphylococcus aureus.

S.No	Name of the test organism	Name of thetest sample	Zone of inhibition (mm) Mean±SD				
			500 µg/ml	250 µg/ml	100 µg/ml	50 µg/ml	PC
1.	E.coli	ZnO+Extract	13.5±0.70	5.25±0.35	0	0	16±1.41
2.	Staphylococcus aureus		12.75±1.06	0	0	0	17.5±0.7

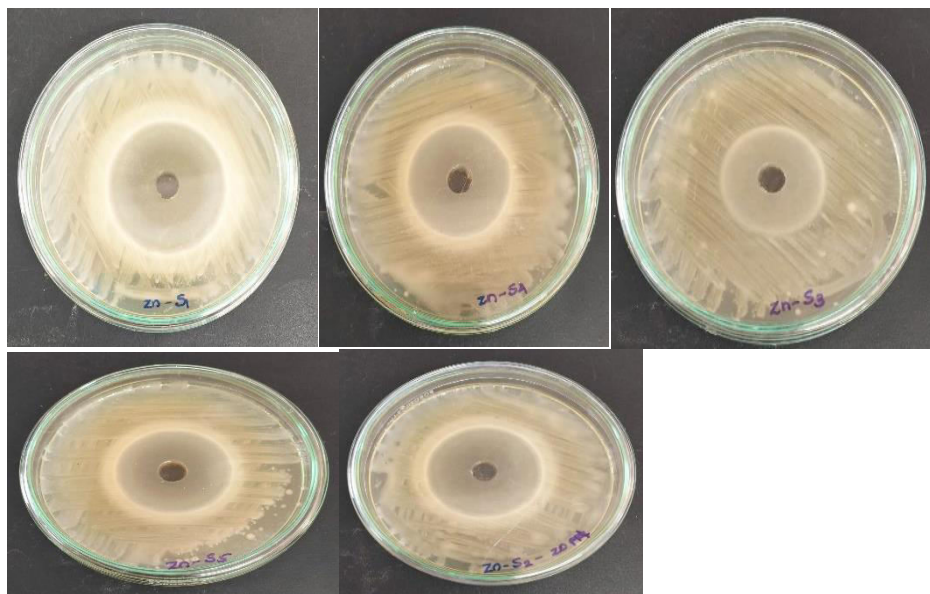SD – Standard Deviation, *Significance - $p < 0$

Fig 7. Anti-bacterial activities of ZnO nanoparticles with neem flowersextract

Table 2Antibacterial activities on gram positive pathogens

   1. **Staphylococcus (+ve)**

Sl no	Name of the plate	Zone of inhibition (cm)
1	Zn-S1	2.06±0.05
2	Zn-S2	2.06±0.05
3	Zn-S3	1.83±0.05
4	Zn-S4	2.20±0.10
5	Zn-S5	1.96±0.11

Table 3Antibacterial activities on gram negative pathogens

   2. **Klebsilla (-ve)**

Sl no	Name of the plate	Zone of inhibition (cm)
1	Zn-S1	1.76 ±0.05
2	Zn-S2	1.74±0.05
3	Zn-S3	1.40±0.10
4	Zn-S4	1.50±0.10
5	Zn-S5	1.50±0.10

From table 2 and 3, it was observed that the maximum ZOI was obtained for gram positive pathogens and gram negative pathogens even taken very low level of ZnO NPs with neem flowers extract[28].

3.3.3Antifungal activity

The anti-fungal agent present in the given sample was allowed to diffuse out into the medium and interact in a plate freshly seeded with the test organisms. The resulting zones of inhibition will be uniformly circular as there will be a confluent lawn of growth. The diameter of zone of inhibition can be measured in millimeters.The potato dextrose agar medium was prepared by dissolving 20 gm of potato influsion, 2 gm of dextrose and 1.5 gm of agar in 100ml of distilled water. The dissolved medium was autoclaved at 15 lbs pressure at 121°C for 15 minutes. The autoclaved medium was mixed well and poured onto 100mm petri plates (25-30 ml/plate) while still molten. Petri plates containing 20ml potato dextrose agar medium was seeded with 72 hr culture of fungal strain (Candida albicans, Aspergillus niger) with different concentration of sample A (500, 250, 100 and 50 µg/ml) was added. The plates were then incubated at 28°C for 72 hours. The anti-fungal activity was assayed by measuring the diameter of the inhibition zone formed around the wells. Amphotericin B was used as a positive control. The values were calculated using Graph Pad Prism 6.0 software (USA).

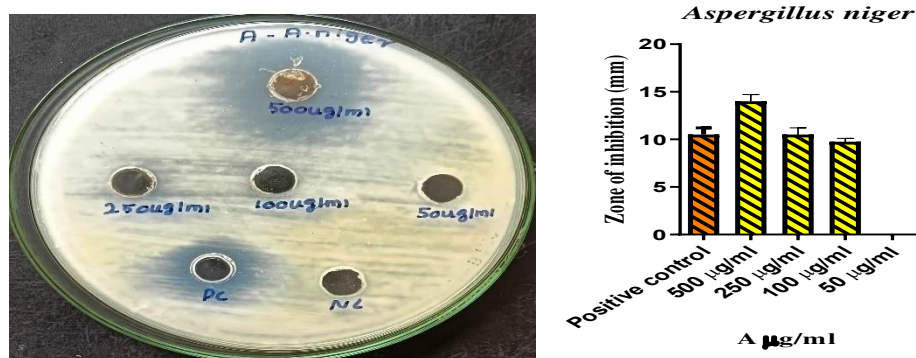**Fig 8. Effect of sample A against Candida albicans.**

Fig : 9 Effect of sample A against A.niger.

Table 4.SD± Means of zone of inhibition obtained by sample A against Candida albicans , Aspergillus niger.

S.NO	Name of the test organism	Name of the test sample	Zone of inhibition (mm) SD ± Mean				
			500 µg/ml	250 µg/ml	100 µg/ml	50 µg/ml	PC
1.	Candida albicans	A	14.5±0.70	10.25±1.06	10±0.70	8.5±0	10.25±0.35
2.	Aspergillus niger	A	14±0.70	10.5±0.70	9.75±0.35	0	10.5±0.70

SD – Standard Deviation, *Significance - $p < 0.05$

3.3.4 Mechanism of Photocatalytic reaction

The general mechanism of photocatalytic reaction is shown in the below figure 9(a) and figure 9(b).The electron in conduction band and hole in valence band are move towards the catalyst surface, participate in surface reactions to give oxidizing species. Thhis reaction takes placeaccording to Langmuir theory of unimolecular adsorption, photogenerated oxidizing species are confined to the surface of photocatalyst and they are unable to move far from it. This causes photocatalytic degradation takes place at the surface (or)it can be within a few monolayers around it [28]. A similar mechanism of photocatalytic degradation of methylred are shown in figure 9(a) and figure 9(b)
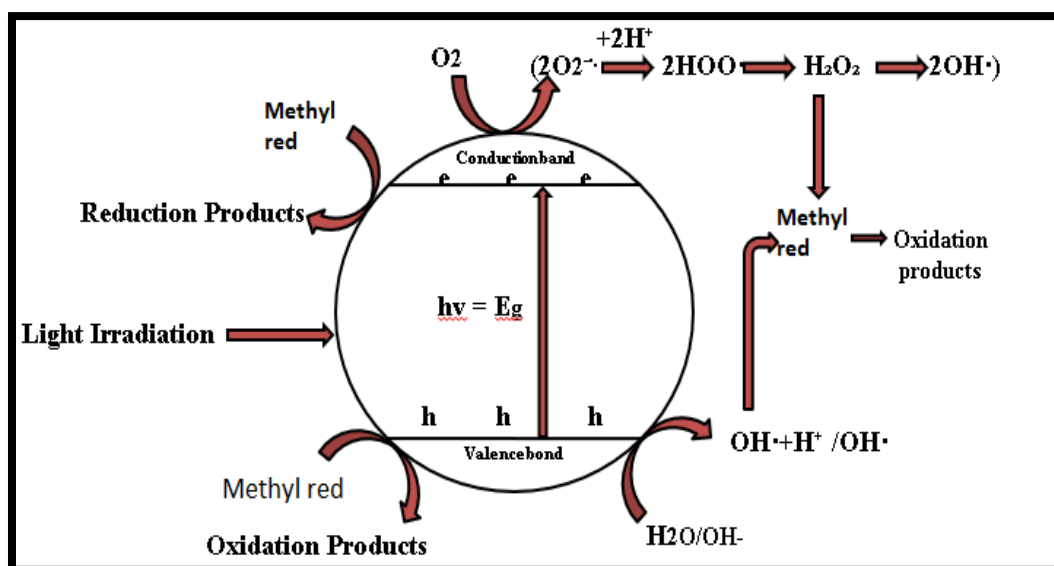

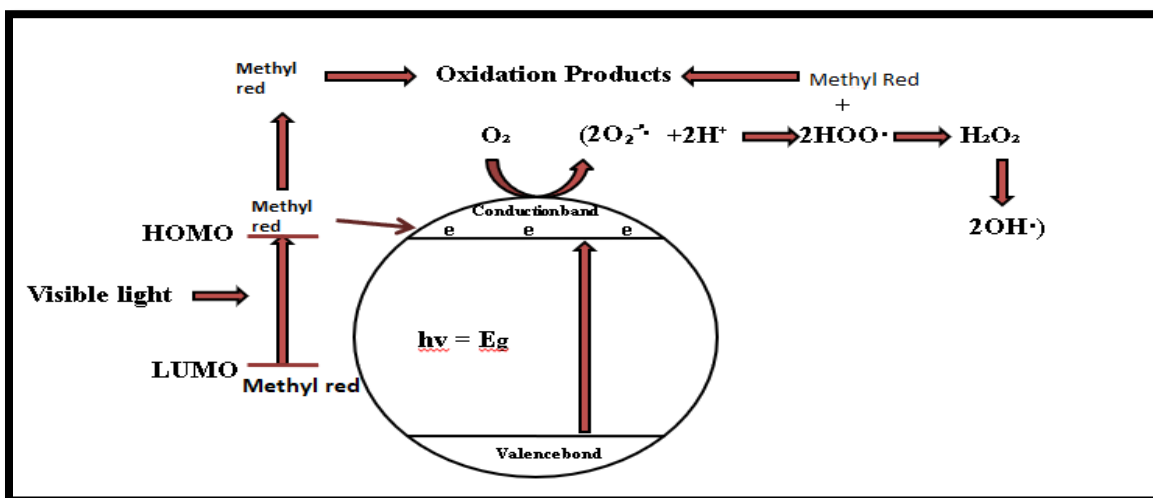**Fig9 (a) .Photocatalytic Activity Reaction (a)**

Fig9 (b). Photocatalytic Activity Reaction (b)

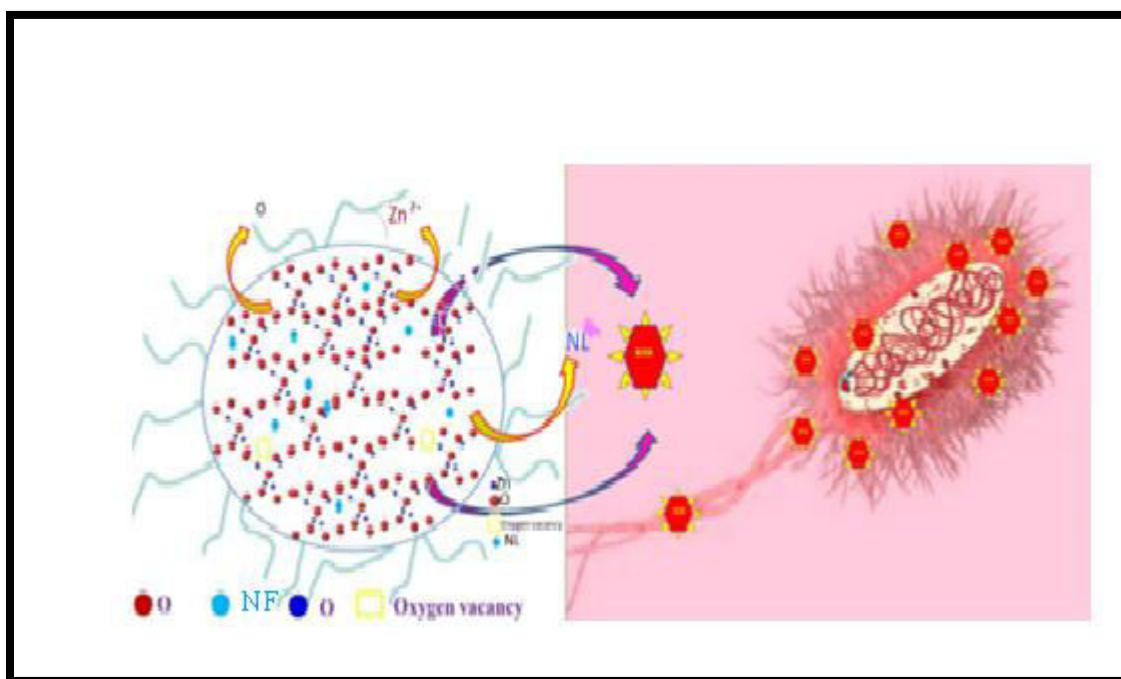### 3.3.5. Mechanism of anti bacterial and antifungal activities

Fig 10. The possible mechanism ofZnONPs using Neem flowers extracts on fungi.
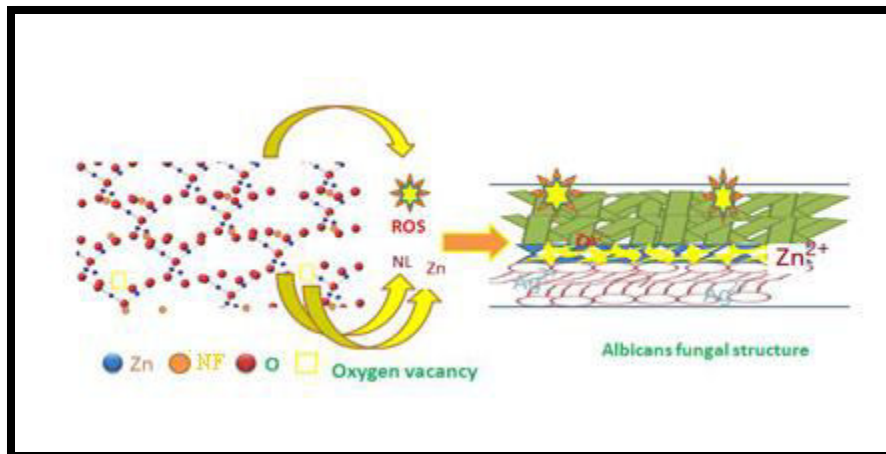
**Fig 11. Depiction of possible mechanism of ZnONPs using Neem flowers extracts on fungi.**

The antibacterial activities offlower extracts molecules incorporated ZnONPswere investigate during the agar well diffusion method using on Mueller-Hinton agar (MHA) for a Gram Positive (staphylococcus aureus) and a GramNegative(Escherichia coli) bacteria.MHA agar plates were inoculated with bacterial strain under aseptic conditions and wells ofdiameter6 mmcontainingthe 3 : 1 M samples(50 µl) were separated as 100µg/ml,250µg/mland 500µg/mlplaced on the agar and incubated at 37°C for 24 hours where bacteria are growing. To distinguish purpose from its sample effect, gentamicin,a standard antibioticis used as a control. The zone of inhibition (ZOI) was observed by evaluating the diameters of the inhibition zones around the wells. The antibacterial activities of Nanoparticles samples were tested against two different bacteria viz.staphylococcus aureus (Grampositive)andEscherichia coli (Gramnegative) using well diffusion method and the digital snapsshowing the ZOI around the wells are shown infigure 9andfigure10. From these results, it is found that ZnO+ Neem flowers extract nanopowder exhibits the highest antibacterial efficiency against both the bacteria when compared with four different percentage of samples where even sample of with lower concentration of NPsshows the remarkable ZOI[29–31]. The general mechanism of antifungal activity is shown in figure s 10 and 11..

Different zone of inhibition with diameter in mm of the antibacterial active percentage of the green synthesized ZnO + Neem leaf extracts is better thanothers. TheantibacterialefficiencyofZnO+NFEnanopowderisgenerallydeterminedbythefollo wingthreefactorsas follows (a)percentageofreactiveoxygenspecies(ROS), (b) percentageofZn $^{2+}$ ions (c) geometrical nature of particles and its volume. According to electromagnetic waves fundamental concepts, if a required amount of light energy which is approximately match with the value of energy gap is interact with green synthesized nano particles, due to the electronic excitation of an
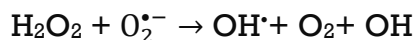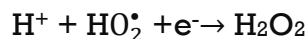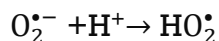
electron from the lower energy level to higher energy levels say valence band (VB) to conduction band (CB) happened releasing aholeintheVB is represent as follow:

ZnO+NFE extracts + $h\nu \rightarrow h^+ + e^-$

$$O_2 + e^- \rightarrow O_2^{\bullet -}$$

The electrons at higher energy levels (CB) as well as holes formed in the lower energy level (VB) produced such as hydrogen peroxide (i) hydroxyl radical ions (HRI) (ii) reactive oxygen species (ROS), super oxide anion $(O^\bullet)^-$ (SOA) in the environment of interaction sample and microbe as written in the following equations.

$H^+ + H_2O \rightarrow OH^\bullet + H^+$

$O_2 + e^- \rightarrow O_2^{\bullet -}$
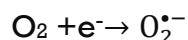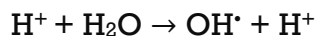
The ROS making the rupture of cell membrane as a result of dissociation of DNA, pilus, plasmid, ribosome, cytoplasm, cytoplasmic membrane, cell wall, capsule, nucleoid, and flagellum and this leads to the bacteria in active condition or totally broken into many pieces. Moreover, ZnO+NFEnanopowder, ROS are produced when the holes interaction with the $O_2^{\bullet -}$ which are represented as follows in the simultaneous manner.

$$O_2^{\bullet -} + H^+ \rightarrow HO_2^\bullet$$
$$H^+ + HO_2^\bullet + e^- \rightarrow H_2O_2$$

$H_2O_2 + O_2^{\bullet -} \rightarrow OH^\bullet + O_2 + OH$

The following proposed mechanism is applicable for all various proportions in percentage ZnO + NFEnanopowder. In the first step, the participation of some ions and oxides during this interaction is emanated according to Haber–Weiss reaction theory where hydroxyl and hydroxide ions are generated from the reaction of H_2O_2 and superoxide ion. Out of these H_2O_2 and ROS, H_2O_2 makes abnormal dissociation when interact with bio parts of the bacteria. As these results, $OH^\bullet$ radicals is liberating when H_2O_2 reacts with SOA($:O_2^{\bullet -}$). The greater number of 'O' vacancies exist in the case of entitled NPs are larger when compared with other. The immediate association of phytochemicalswith releasing of simple ions into the ZnO + NFE is supposed to be the responsible for the generation of a greater number ofoxygen vacancies in the nanoparticles. As consequence of this, more number of Zn^{2+}ionsreleasedfromthesurfaceofthenanopowder execute the bacteria colony vanishing due to the strongelectrostatic force of attraction between the positively charged ionsand negativelychargedcytoplasmic membrane of cell ofthebacteria.
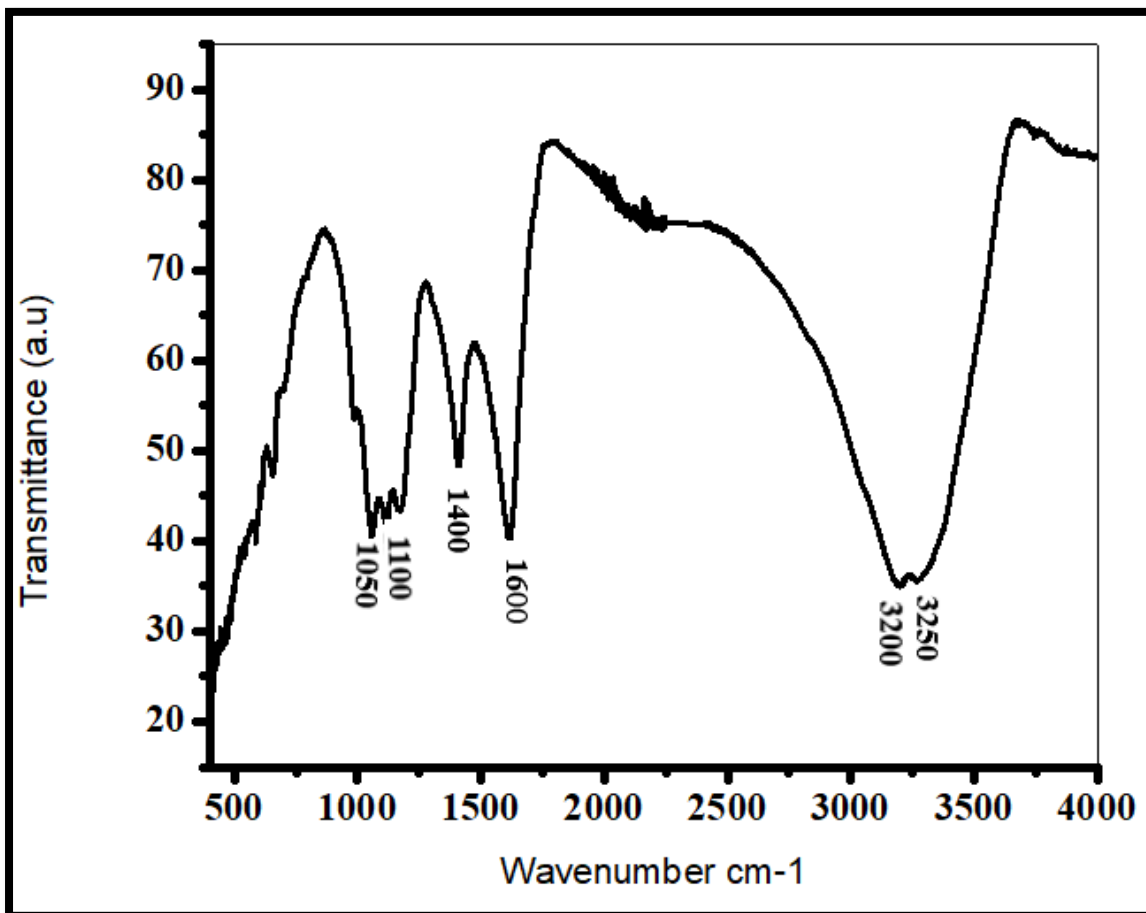
4.FT-IR Analysis

Fig12. FT IR Spectrum of ZnO nanoparticles with neem flowers extract

IR spectrum belongs to 545 Cm^{-1}belongs toZnO nanoparticles. The broad peak belongs to 3250 belongs to OH stretching vibrations. The broad spectrum at 1600 Cm^{-1}belongs to N-H stretching vibrations, 1482 Cm^{-1}belongs to monosubstituted alkynes,.1100Cm^{-1}denotes C-O-C linkages or C-O bonds.
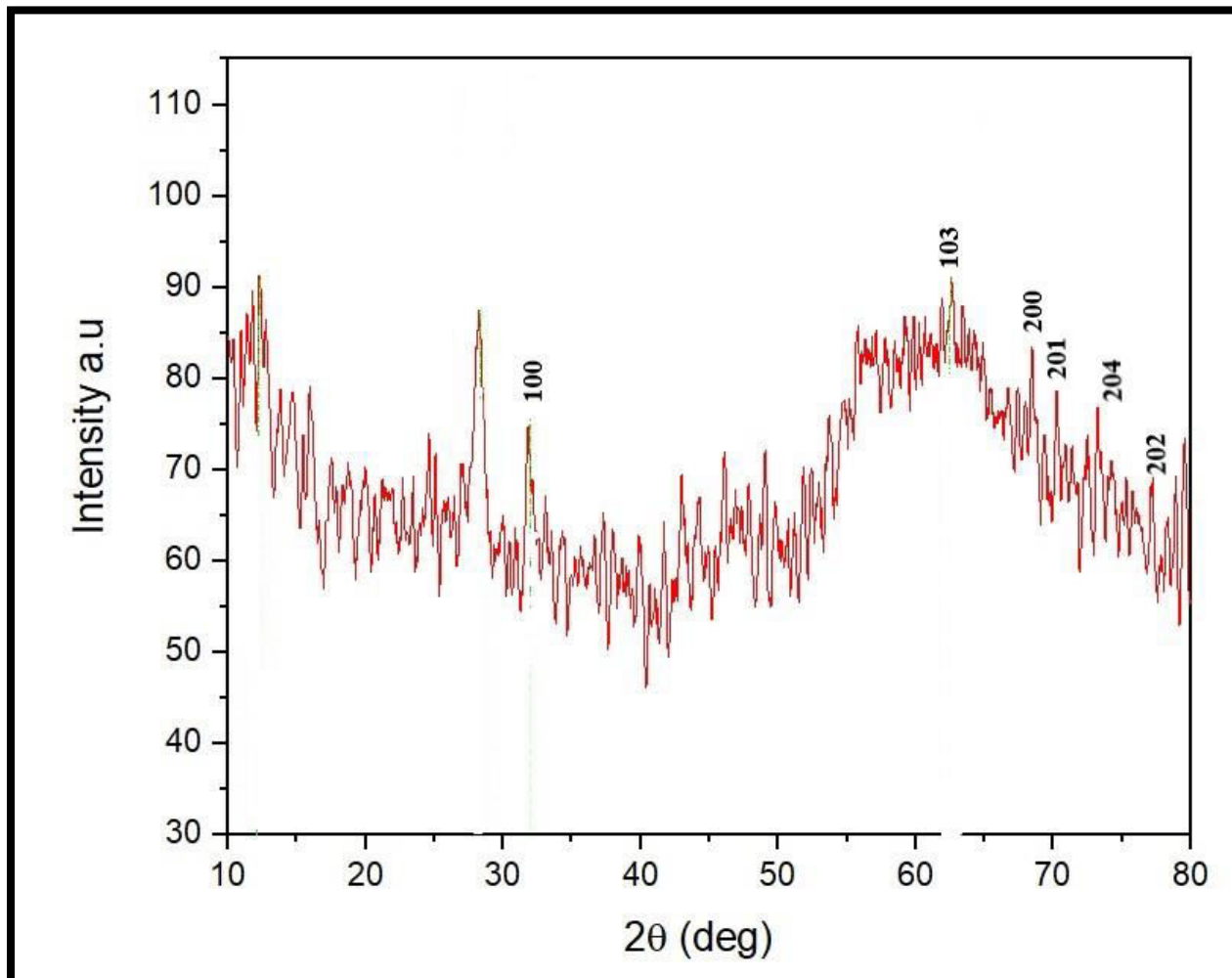
5.XRD Analysis

Fig13. XRD analysis of ZnO nanoparticles with neem flowers extract

An intense method of X-ray powder diffraction (XRD) was utilized to discover the crystalline phase which is available in materials. It is also useful to measure the structural properties of those phases. X-ray powder diffraction patterns of the pure and the ZnOwithneem leaf extract nanoparticles are shown in Fig.12. The excellent peaks (100), (103), (200) (201,)(202),(204) were obtained. ZnO nanoparticles size has been determined using the Scherrer formula:

$$D = 0.9\lambda/\beta \cos \theta \text{--------------(2)}$$

where λ is the X-ray wavelength, θ is the Bragg diffraction angle and β is the full width at half maximum (FWHM) of the XRD peak appearing at the diffraction angle θ.

The grain sizes were evaluated from the Scherrer's relation. It showed that increases in the dopant concentration of ZnO increased the average grain size. XRD analysis proves that crystalline structure of ZnO asWurtzite and those peaks are seen at

32°,68°,70°,72°,78°,62° due to the diffraction planes are in good agreement with [JCPDS.No.01-079-2205]It hashexagonal structure.

6.SEM-EDAX

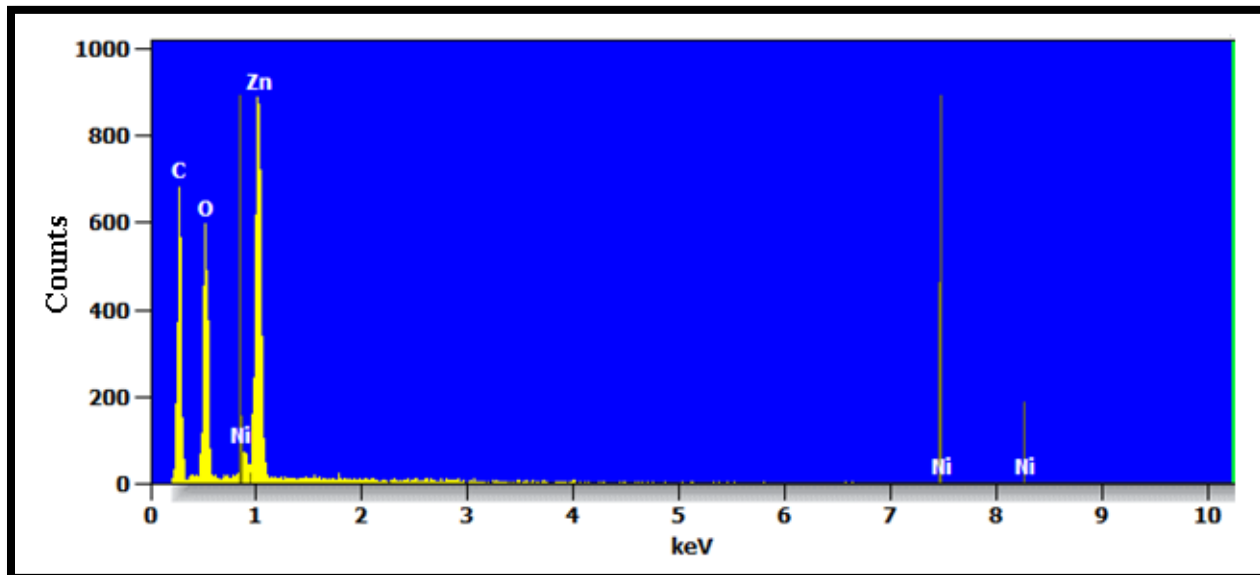**Fig14. SEM -EDAX analysis of ZnO nanoparticles with neem flowers extract**

Scanning electron microscopy (SEM) is one of the most widely used techniques for the characterization morphology of the particles. The SEM pictures of the pure and the ZnO-dopednanoparticles with neem leaf extract are shown in Figure 14. It is clearly observed that the particles that are highly aggregated are of permeable nature. There are small agglomerated particles and this may be because of the lower calcination temperature. This affirms the decrease in crystalline size essentially by adding ZnO nano particles to extract[32].
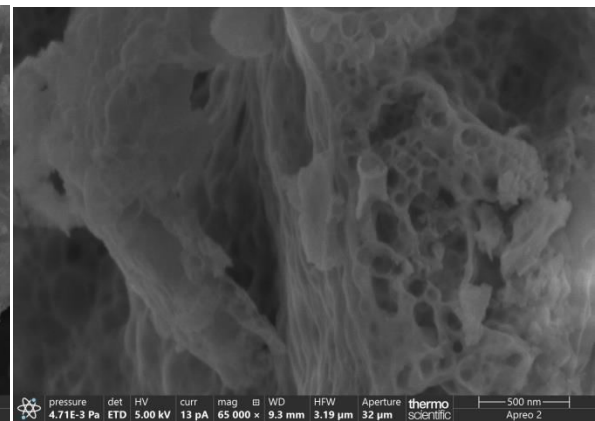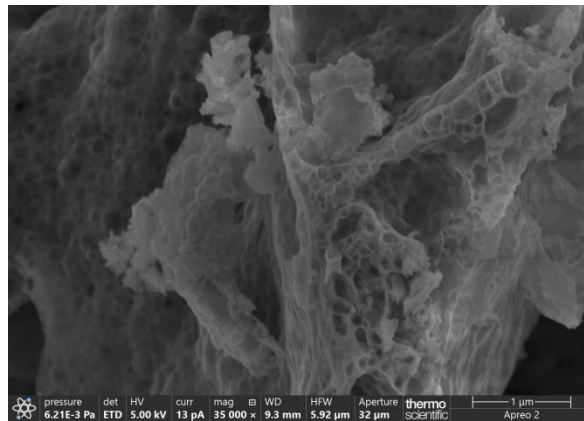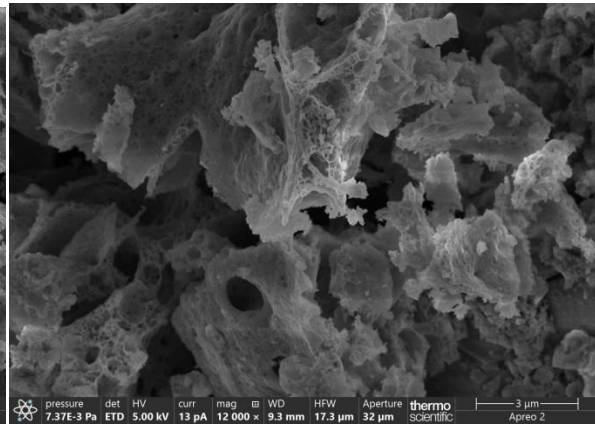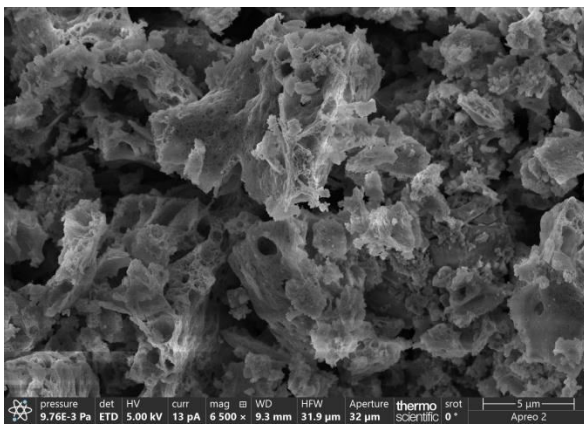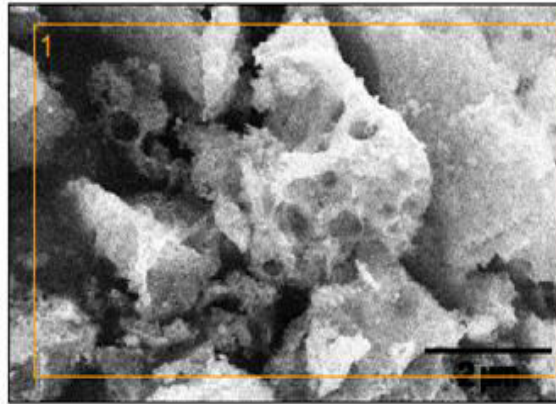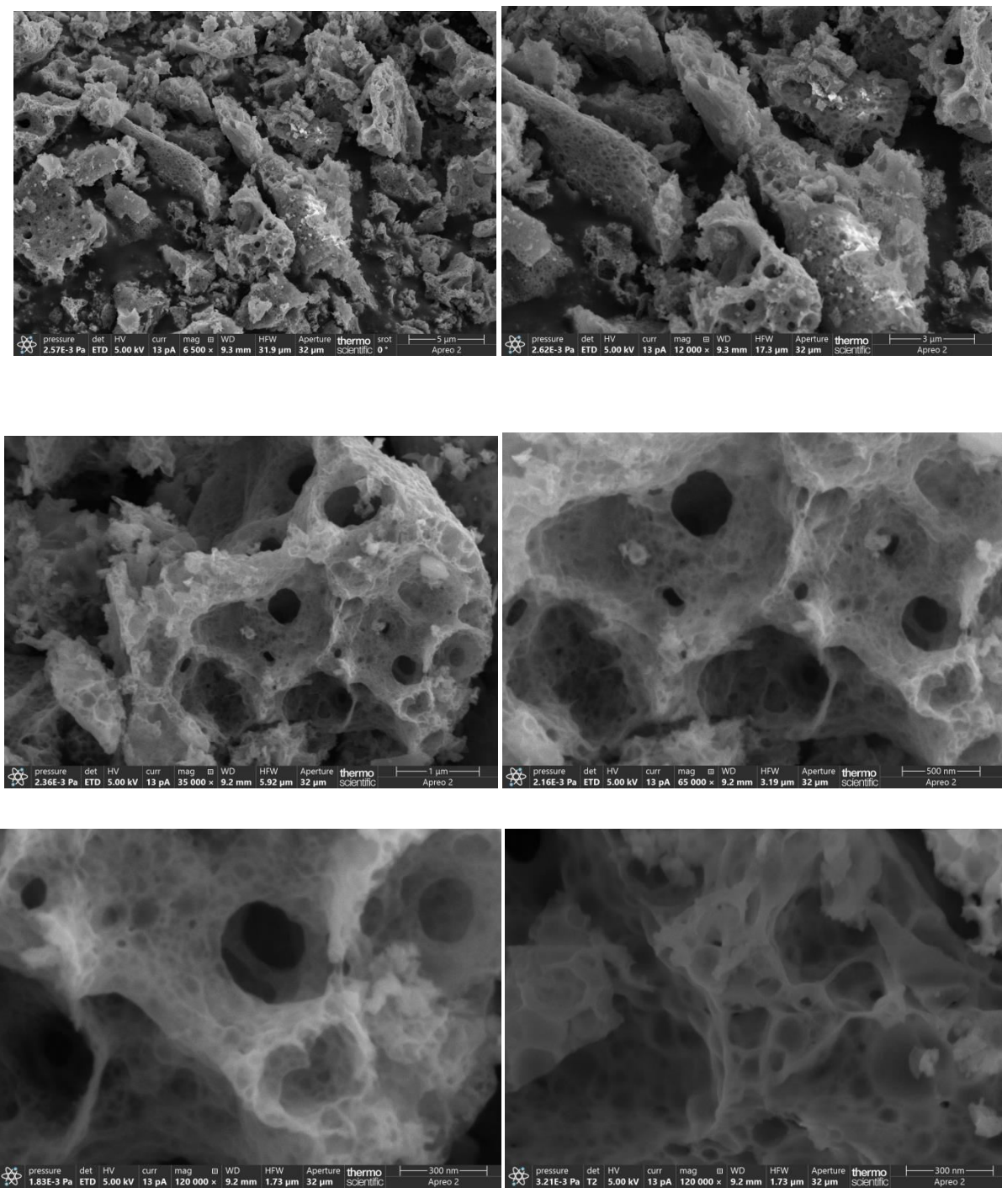
Fig 15. Various SEM micrographs ofZnONPs with Neem flowers extract

Table 5EDAX analysis of ZnONPS with Neem flowers extract

Element	Net counts	Weight %	Atom%
C	3122	23.29	44.39
O	2961	26.56	38.01
Ni	105	0.92	0.36
Zn	6507	49.2	17.24
Total		100.0	100.0

The presence of composition elements like Carbon (Cu), Nitrogen(N),Oxygen(O) Nickel(Ni), Zinc (Zn), were confirmed by EDAX analysis..The weight composition obtained from EDAX analysis of the normalized spectrum was Zn and oxygen.. EDAX also revealed the formation of Zn dopedwith neem flowers extract NPs with oxygenand with Zn which shows better antibacterial activity.

7. Conclusion

It is concluded that ZnO NPs with neem flowers extract have better antimicrobial and antifungal activity when compared to other metal oxide NPs. It has the potential of good photo degradation activity in methyl red medium of 2M ZnONPs with NFE. These activities are supported bycharacterisation techniques of UV, XRD,SEM,EDAX FT-IR , Agarwell-diffusion method and disc- diffusion method.

References

1. Wang,Y,;Wang,Z,; Muhammad,S,; and He,J,; CrystEngComm. 2012,14,5065.
2. Higashimoto, S,; Tanaka,Y,; Ishikawa,R,; Hasegawa, S,; Azuma, M,; Ohue,H and Sakata,Y,; Catal. Sci. Technol. 2013,3,400.
3. Trovarelli,A,;   De Leitenburg, C,; Boaro,M,;and   Dolcetti, G,;Catal. Today.1999,50,353.
4. Li,R,X,; Yabe,S,;   Yamashita,M,;   Momose,S,; Yoshida,S,; Yin,S,; and Sato,T,;Solid State Ion.2002,151, 235.
5. Masui,T,;   Hirai,H,; Hamada,R,; Imanaka,N,; Adachi,G,; Sakata,T,; and Mori,H,;J. Mater. Chem. 2003,13,622.

6. Liu,I,;Hon,M.H.; and Teoh,L.G,; J. Electron. Mater.2013, 42, 2536.

7. Saranya, J,;Ranjith,K.S,; Saravanan,P,; Mangalaraj,D,; and Rajendra Kumar,R.T,; Mater. Sci. Semicond. Process.2014,26,218.

8. Herrling,T,; Seifert ,M,;andJung,K,; SOFW J,;2013,12,139.

9. Pouretedal,H,R,; and Kadkhodaie,A,; Chin. J. Catal.2010,31,1328.

10. Mohamed,R,M,; and Aazam,E,S,; Int. J. Photoenergy, Article ID 137328 2011.

11. Sifontes,A,B,; Rosales,M,; Méndez,F,J,; Oviedo,O,; and Zoltan,T,J,;2013,1. Nanomater., 2013, 1 (2013);

12. Akbari-Fakhrabadi, A,; Saravanan,R,; Jamshidijam, M,; Mangalaraja,R,V and Gracia,M,A,; J. Saudi Chem. Soc.2015,19,505.

13. Li,W,; Liang,R,; Hu,A,; Huang,Z,; and Zhou,A,N,; RSC Adv.2014,4,36959.

14. Liyanage,A,D,; Perera,S,D,; Tan,K,; Chabal,Y,; and Balkus,K,J,; Jr. ACS.2014,4,457.

15. Channei,D,;Inceesungvorn,B,; Wetchakun,N,; Ukritnukun,S,; Na ttestad,A,; J. Chen and S. Phanichphant, Sci. Rep.2014,4, 5757.

16. Primo,A,; Marino,T,; Corma,A,; Molinari,R,; and García, H,;J. Am. Chem.2011,133,6930

17. Liang,H,;Raitano,J,M,; He,G,; Akey,A,J,; Herman,I,P,; Zhang,L,; and Chan,S,W,; J. Mater. Sci.2012, 47, 299.

18. Tan,J,;Zhang,W,; Lv,Y,H,; and Xia,A,L,; Mater. Res.2013, 16, 689.

19. Yue,L.; and Zhang,X,M,; J. Alloys Compd.2009, 475, 702.

20. .Montini,T,;Melchionna,M,; Monai,M,; and Fornasiero,P,; Chem. Rev.2017,116,5987.

21. Herrera, F,; Kiwi, J,; Lopez,A,; and Nadtochenko,V,; Environ. Sci. Technol.1999,33,3145.

22. A.Nadhman, et al., PEGylated silver doped zinc oxide nanoparticles as novel photosensitizers for photodynamic therapy against Leishmania, Free Radic. Biol. Med.2014, 77, 230–238.

23. S. Ahmed, S.A. Chaudhry, S. Ikram, A review on biogenic synthesis of ZnO nanoparticles using plant extracts and microbes: a prospect towards green chemistry, J. Photochem. Photobiol. B Biol. 2017,166, 272–284.

24. DDodoo-Arhin,T.Asiedu,B.Agyei-Tuffour,E.Nyankson,D.Obadaa,J.M.Mwabora. Photocatalytic degradation of Rhodamine dyes using Zinc Oxide nano particles, Volume 38,Part 2,2021, 809-815.

25. Choudhary,B,P,; Rai,S,; Singh,N,B,; Green synthesis of pure and silver doped copper oxide nanoparticles using Moringa oleifera leaf extract. Emerg Mater Res.2017, 6,285–295.

26. Tachikawa,T, Fujitsuka,M,; and Majima,T,; J. Phys. Chem. C,2007, 111, 5259.

27. Sun,Y,;Qu,B,; Liu,Q,; Gao,S,; Yan,Z,; Yan,W,; Pan,B,; Wei,S,; and Xie,Y,; Nanoscale.2012, 4, 3761. https://doi.org/10.1039/c2nr30371j.

28. Chatti,M,;Adusumalli,V,N,K,B, S,; Ganguli and Mahalingam,V,; Dalton Trans.2016, 45, 12384.

29. Amiri,M,R,; Alavi,M,; Taran,M,; Kahriz,D,; Antibacterial, antifungal, antiviral, and photocatalytic activities of TiO2 nanoparticles, nanocomposites, and bio-nanocomposites: recent advances and challenges. J Public Health Res2022,7,1–6.

30. Sankar,R,;Manikandan,P,; Malarvizhi,V,; Fathima,T,; Shivashangari,K,S,; Ravikumar,V,; Green synthesis of colloidal copper oxide nanoparticles using Carica papaya and its application in photocatalytic dye degradation. Mol BiomolSpectroscSpectrochim Acta Part A. 2014,121,746–750.

31. Sheikh,M,C,; Hasan,M,M,; Hasan,M,N,; Salman,M,S,; Kubra,K,T,; Awual, M,E,; Waliullah,R,M,; Rasee A,I,; Rehan,A,I,; Hossain,M,S,; Marwani,H,M,; Islam,A,;Exploring moisture adsorption on cobalt-doped $ZnFe_2O_4$ for applications in atmospheric water harvesting 2024, 14, 6165-6177.

32. Khaleque,M.S,;Awual,M,R,; Toxic Chemistry Africa cadmium (II) monitoring and removal from aqueous solution using ligand-based facial composite adsorbent. J Mol Liq.2023, 389,122854.